

Supplementary Material

Interpenetrated Double Pillared-Layer Co^{II} MOFs with pcu Topology

*In-Hyeok Park,^A Yunji Kang,^A Eunji Lee,^A Anjana Chanthapally,^B
Shim Sung Lee,^{A,C} and Jagadese J. Vittal^{B,C}*

^ADepartment of Chemistry and Research Institute of Natural Science, Gyeongsang National University, Jinju 52828, South Korea.

^BDepartment of Chemistry, National University of Singapore, 3 Science Drive 3, Singapore 11753, Republic of Singapore.

^CCorresponding authors. Email: sslee@gnu.ac.kr; chmjv@nus.edu.sg

Table S1. Crystal data for **1-3**. CCDC numbers 1495679 -1495681

	1	2	3
formula	C ₅₉ H ₅₃ Co ₂ N ₅ O ₁₂	C ₆₄ H ₄₄ Co ₂ N ₄ O ₈	C _{75.50} H _{73.50} Co ₂ N _{6.50} O _{14.50}
formula weight	1141.92	1114.89	1421.76
crystal system	triclinic	triclinic	monoclinic
space group	<i>P</i> $\bar{1}$	<i>P</i> $\bar{1}$	<i>P</i> 2 ₁ / <i>c</i>
<i>a</i> (Å)	9.9343(9)	12.2506(10)	10.9987(6)
<i>b</i> (Å)	15.3453(16)	16.3861(14)	23.0153(13)
<i>c</i> (Å)	20.229(2)	20.1664(16)	15.1972(9)
α (°)	97.794(4)	104.984(4)	90
β (°)	95.978(4)	91.435(4)	100.015(2)
γ (°)	97.962(4)	91.435(4)	90
<i>V</i> (Å ³)	3001.9(5)	3657.9(5)	3788.4(4)
<i>Z</i>	2	2	2
<i>D</i> _{calc} (g/cm ³)	1.263	1.012	1.246
μ (mm ⁻¹)	0.614	0.499	0.503
2 θ _{max} (°)	52.00	52.00	52.00
reflections collected	48080	88882	23708
independent reflections	4020 (<i>R</i> _{int} = 0.1049)	14360 (<i>R</i> _{int} = 0.0685)	2564 (<i>R</i> _{int} = 0.0675)
goodness-of-fit on <i>F</i> ²	1.064	1.052	1.047
<i>R</i> ₁ , <i>wR</i> ₂ [<i>I</i> > 2 σ (<i>I</i>)]	0.1696, 0.4365	0.0499, 0.1232	0.0765, 0.2204
<i>R</i> ₁ , <i>wR</i> ₂ (all data)	0.2183, 0.4683	0.0842, 0.1314	0.0979, 0.2042

Structural Refinements

Crystal 1

In this structure both bpeb ligands are disordered. Two different models were resolved. They are conformationally disordered with *trans,trans,trans* and *trans,cis,trans* conformations. The occupancies were refined to 0.531(6). Anisotropic refinements of the atoms in the disordered bpeb were having NPD's and hence isotropic thermal parameters were refined. Soft constraints were applied to keep reasonable ideal geometry. The electron densities in the challels were resolved to DMF (0.5, 0.5 and 0.25 occupancies) and some disordered O atoms (3×0.5 and 6×0.25). Soft constraints were applied to keep the geometry ideal for DMF. One carboxyate O atom, O2 is probably disordered but it could not be resolved. Due to the disordered problems, the agreement factors are not very good. We have also attempted to squeeze the data to see if the agreement factors could be improved. But unfortunately, it was realised that the major problem was due to disorders but not the solvent molecules. We have no choice but to leave it as such as we tried to collect the data many times with different batch of single crystals. This is the best we could come up with. In any case, the connectivity of this structure is clearly shown despite poor quality of the model and agreement factors.

Crystal 2

There is no disorder in main frame of the MOF. They behave well. But the guest solvents in the voids are disordered. In the $[\text{Co}_2(\text{ndc})_2(\text{bpeb})_2] \cdot 1.75\text{DMF} \cdot 3.75\text{H}_2\text{O}$ the voids have 3×0.5 and $1 \times 0.25\text{DMF}$ molecules. Soft constraints were applied to keep the ideal geometry. Only isotropic thermal parameters were refined. The small electron densities were assigned to O atoms of the disordered ater in 16 places with occupancies 14×0.25 and 2×0.125 . The H atoms of these water molecules were not added. The final model was not satisfactory due to close to H...H contact in the solvents (A Level Alerts in CheckCIF), hence we resorted to SQUEEZE to complete the refinement which is acceptable.

Crystal 3

In the main structure of the MOF, one bpdc liand was disordered. A common occupancy factor was fined to 0.737(13). For the minor component only isotropic thermal parameter was fined. Hard constraints (AFIX 66) were applied to 6 membered rings. In the voids highly disordered 3.5DMF and 4H₂O were modelled. Soft constraints were applied to keep an ideal geotry of DMF (2×0.5 and 1×0.25). Only isotropic thermal parameters were refined for the minor model with occupancy 0.25. The scattered electron densities were assigned as O atoms of water molecules. They were in 6 positions with occupancies varying from 0.75, 0.5, 2×0.25 to 2×0.125 .

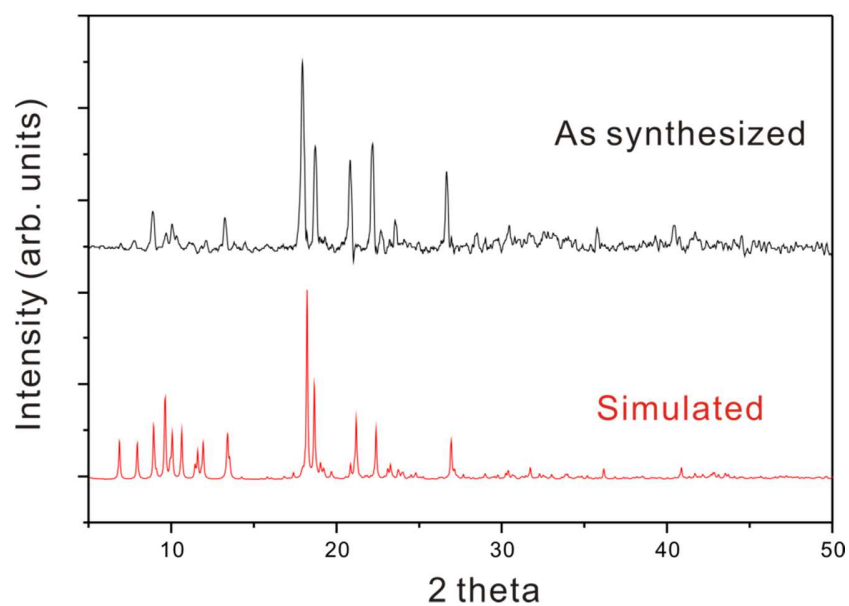


Figure S1. Comparison of PXRD patterns for **1**: (top) as synthesized and (bottom) simulated from the single crystal X-ray data. The deviations in these PXRD patterns may be due to the change of phase due to solvent loss during grinding during sample preparation

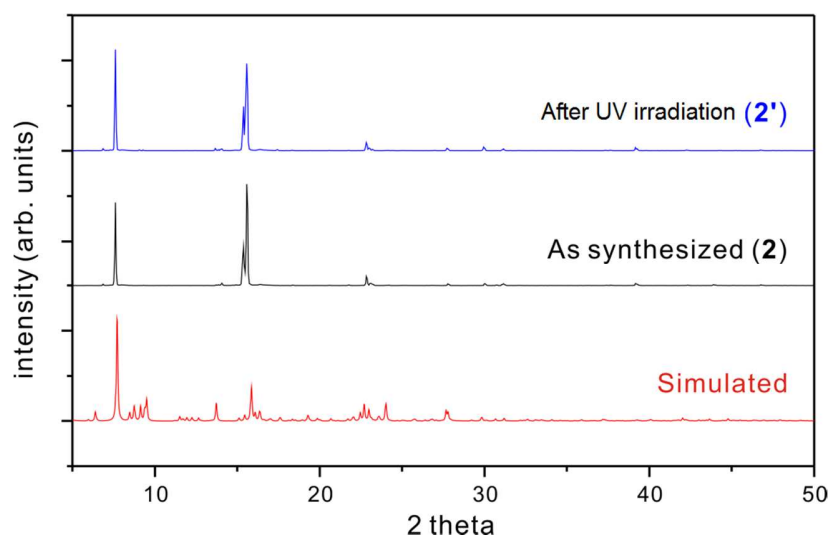


Figure S2. Comparison of PXRD patterns for **2** and **2'** (**2** after UV-irradiated): (top) as synthesized and (bottom) simulated from the single crystal X-ray data. The deviations in these PXRD patterns may be due to the change of phase due to solvent loss during grinding during sample preparation.

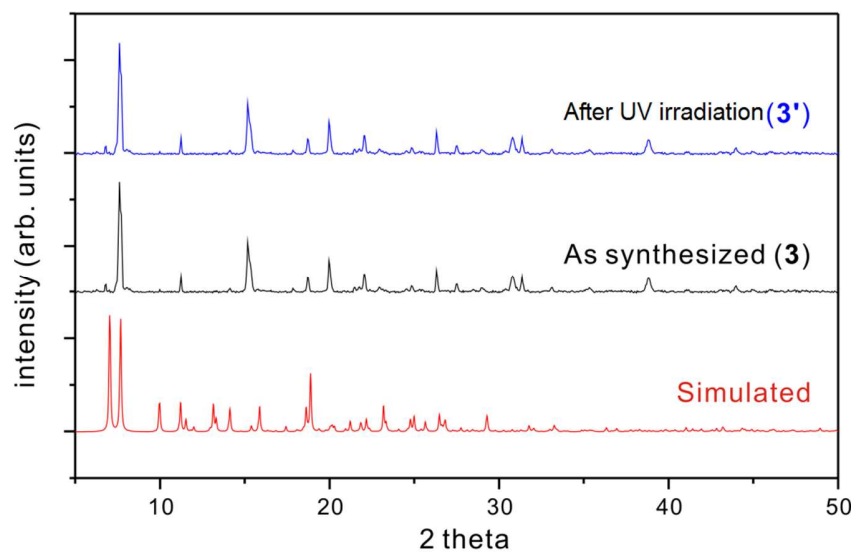


Figure S3. Comparison of PXRD patterns for **3** and **3'** (**3** after UV-irradiated): (top) as synthesized and (bottom) simulated from the single crystal X-ray data. The deviations in these PXRD patterns may be due to the change of phase due to solvent loss during grinding during sample preparation.

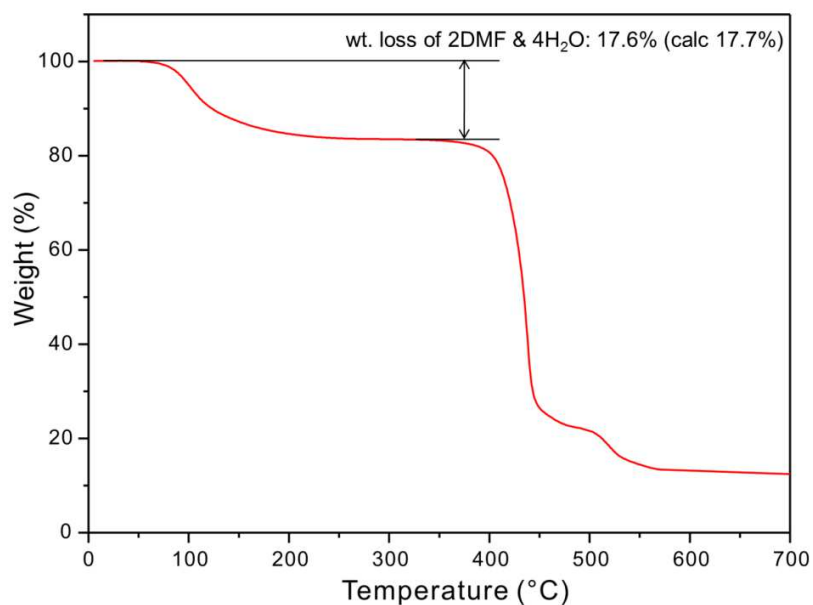


Figure S4. TGA curve of **1** with heating rate of $5^{\circ}\text{C}\cdot\text{min}^{-1}$ under N_2 flow. The desolvated MOF is stable up to 410°C . Please note that the amount of the guest solvents in the single crystals and the bulk are different probably due to handling differently.

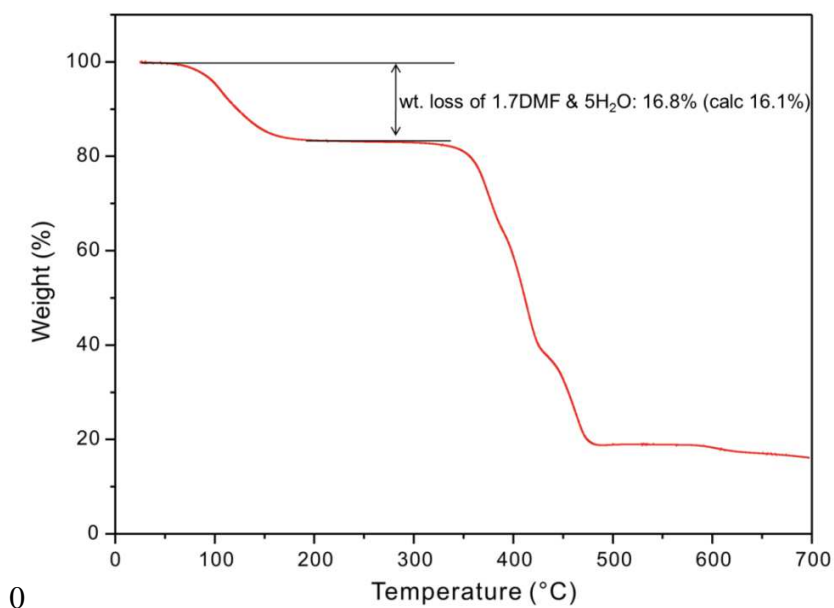


Figure S5. TGA curve of **2** with heating rate of $5^{\circ}\text{C}\cdot\text{min}^{-1}$ under N_2 flow. The desolvated MOF is stable up to 370°C . Please note that the amount of the guest solvents in the single crystals and the bulk are different probably due to handling differently.

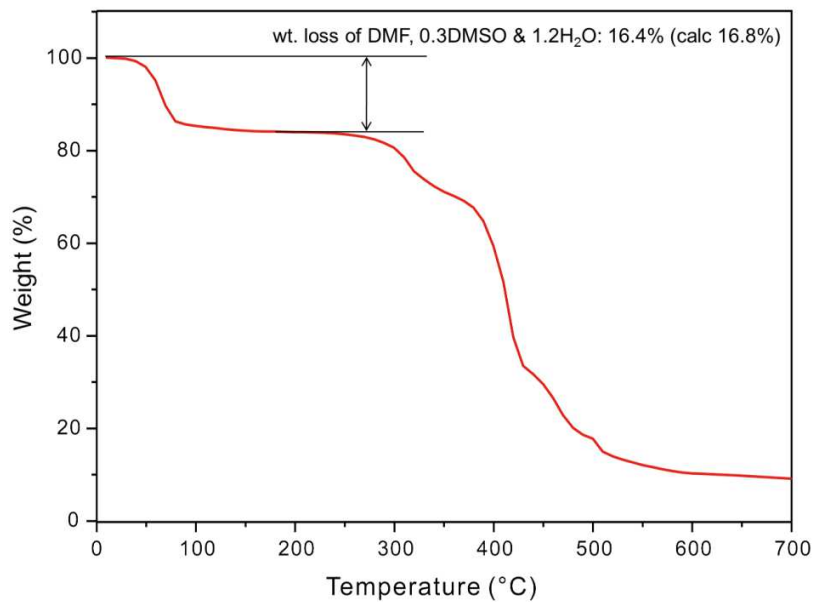


Figure S6. TGA curve of **3** with heating rate of $5^{\circ}\text{C}\cdot\text{min}^{-1}$ under N_2 flow. The desolvated MOF is stable up to 300°C . Please note that the amount of the guest solvents in the single crystals and the bulk are different probably due to handling differently.

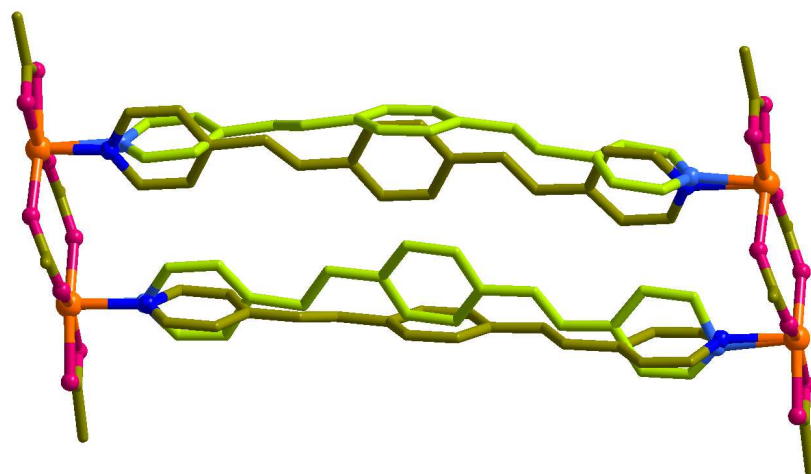


Figure S7. The structure of **1** showing the disorders of bpeb ligands.

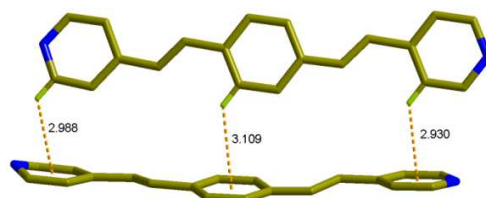


Figure S8. The alignments of two bpeb ligands with *trans,cis,trans* and *trans,trans,trans* conformations in **1** showing three consecutive edge-to-face CH \cdots π interactions.

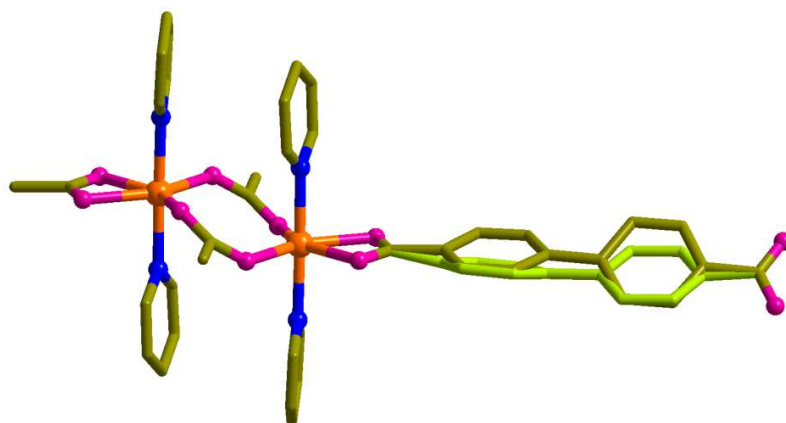


Figure S9. The structure of **3** showing the disorders of bpdc ligand.

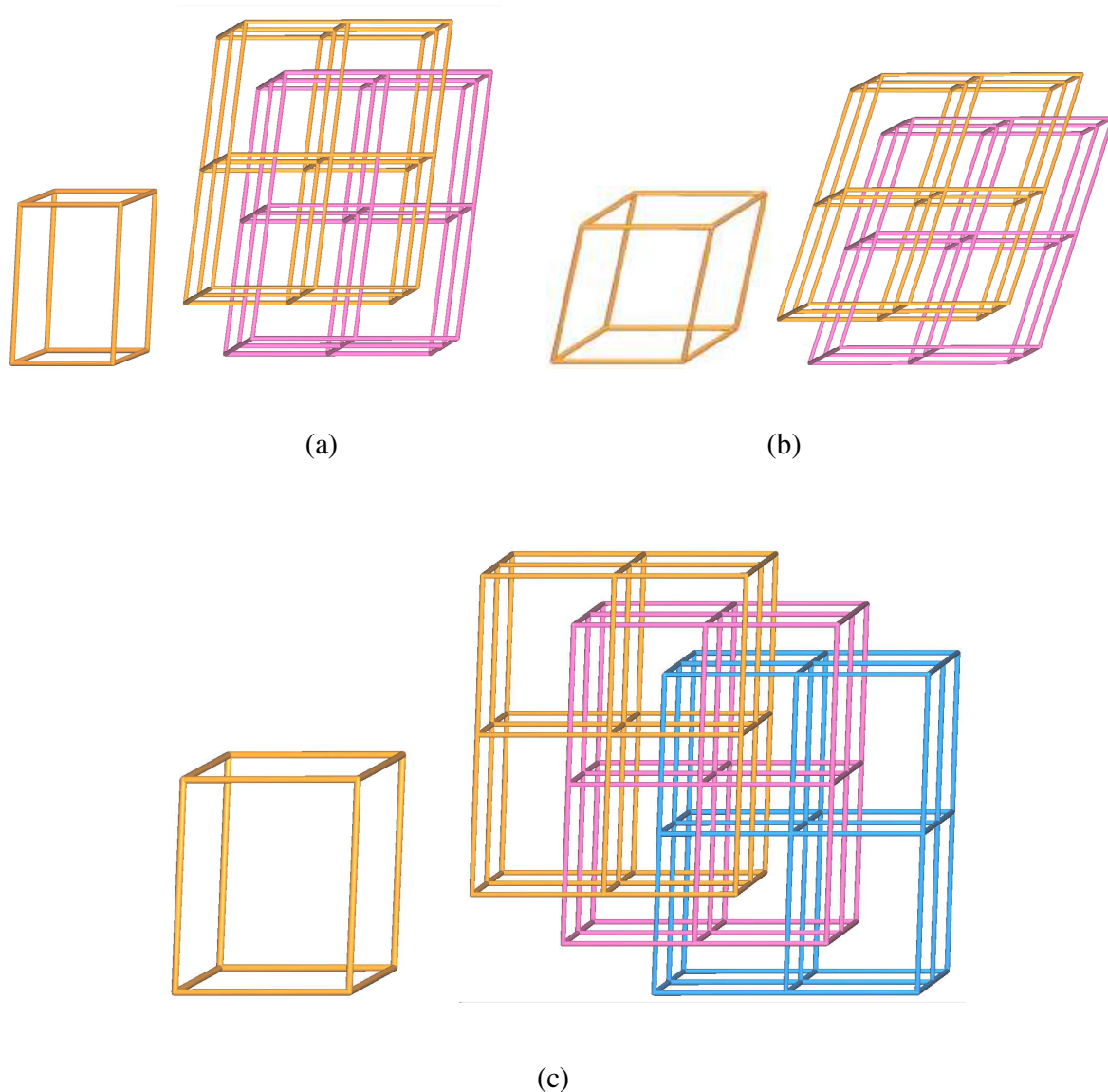


Figure S10. Schematic representations of the **pcu** topologies present (left) and the interpenetrations (right) in (a) **1**, (b) **2** and (c) **3**.

UV Experiments for **2** and **3**.

The UV irradiation experiments were conducted for the samples **2** and **3** in a LUZCHEM UV reactor. Finely powdered samples from single crystals were packed in between the glass slides placed in the UV reactor for 2 days. These glass slides were flipped back at regular intervals of time to maintain the uniform exposure of UV irradiation. After the reaction the $^1\text{H-NMR}$ spectra were recorded (see Figures S11 and S12) and found that both are photo-inert.

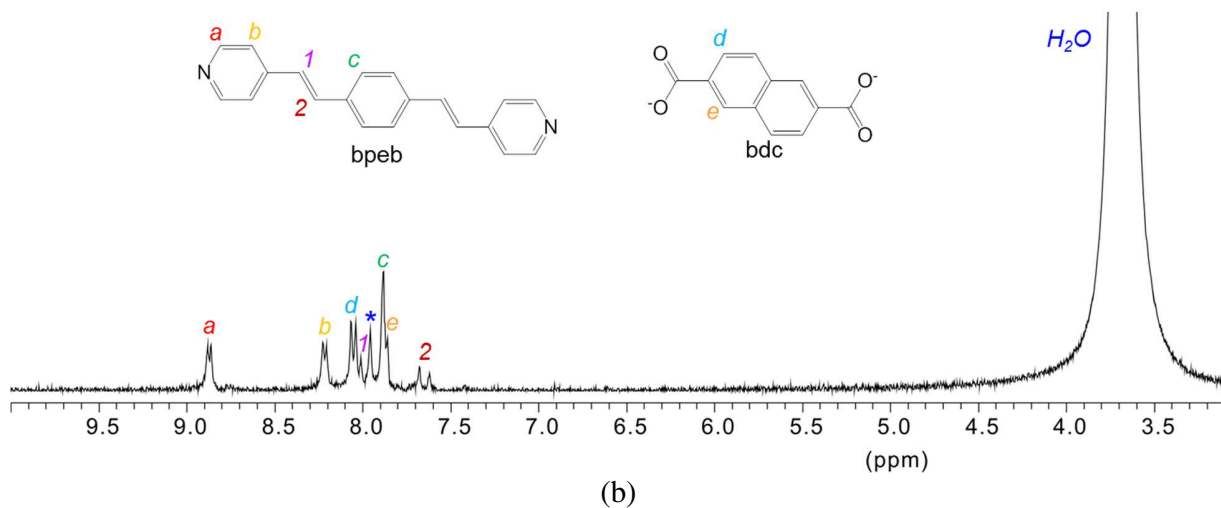
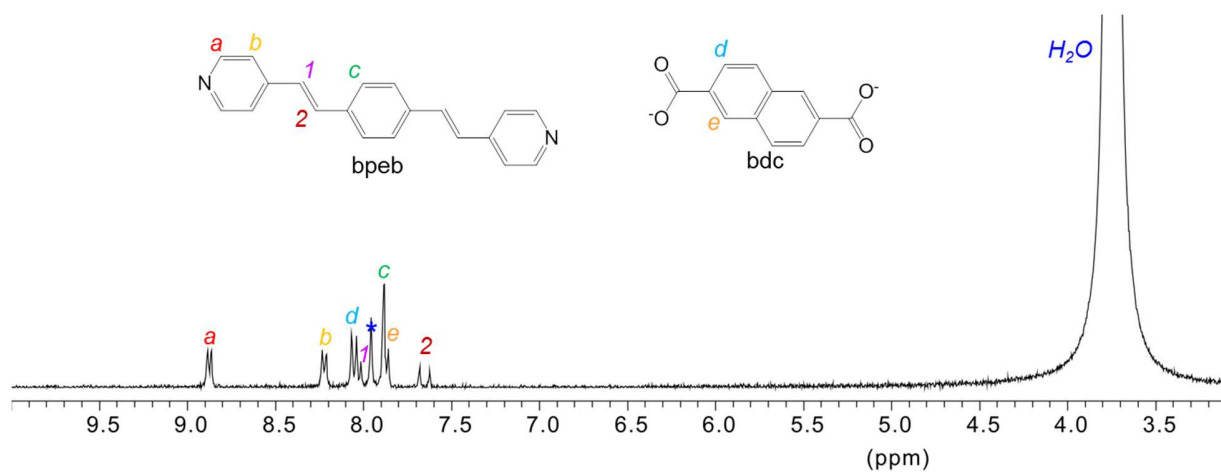
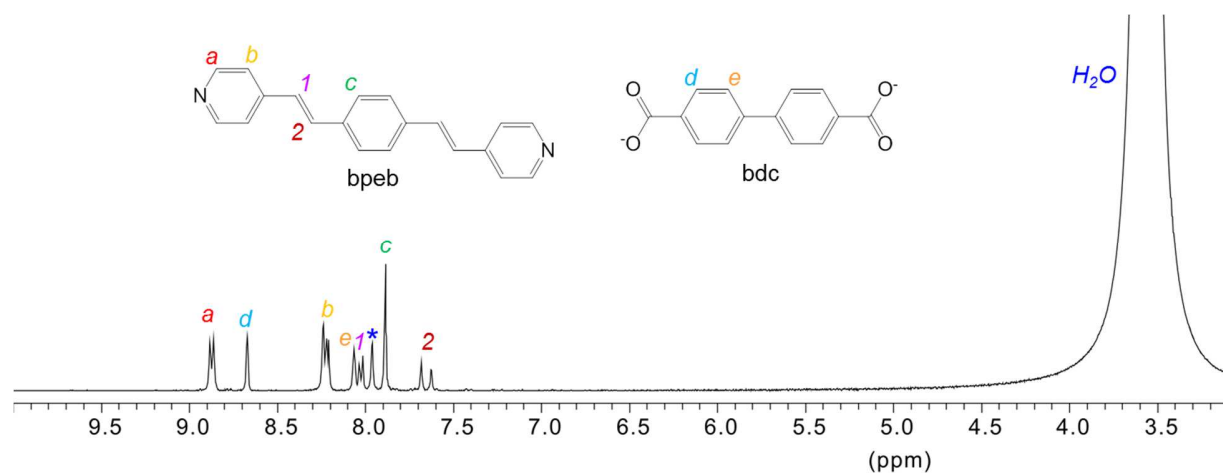
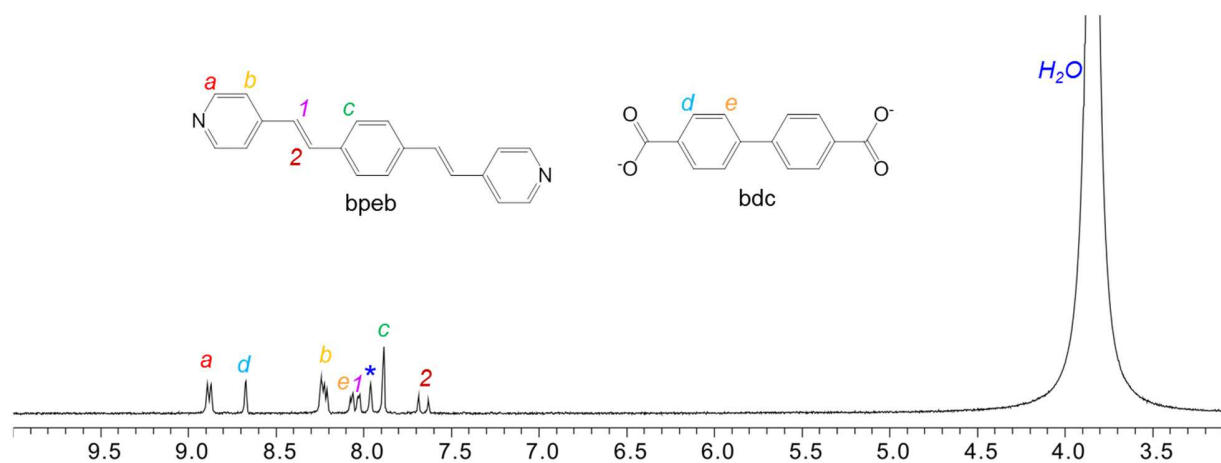


Figure S11. The ^1H NMR spectra of a) **2** and b) **2'** (**2** after UV-irradiated) in $\text{DMSO-}d_6$ with a small drop of HNO_3 to dissolve the crystals. The humps around 3.0 ppm and 4.5 ppm are due to the protonated water in **2** and **2'**, respectively.



(a)



(b)

Figure S12. The ^1H NMR spectra of a) **3** and b) **3'** (**3** after UV-irradiated) in $\text{DMSO-}d_6$ with a small drop of HNO_3 to dissolve the crystals. The humps around 3.0 ppm and 4.5 ppm are due to the protonated water in **3** and **3'**, respectively.